Silver-nano biohybride material: Synthesis, characterization and application in water purification

Dr. Sujoy Das

Bioresource Technology 124 (2012) 495–499

Bioresource Technology 124 (2012) 495–499

Contents lists available at SciVerse ScienceDirect

Bioresource Technology

journal homepage: www.elsevier.com/locate/biortech

Short Communication

Silver-nano biohybride material: Synthesis, characterization and application in water purification

Sujoy K. Das [a,*], Md. Motiar R. Khan [b], Arun K. Guha [b], Akhil R. Das [c], Asit Baran Mandal [a]

[a] Environmental Technology Laboratory, Council of Scientific and Industrial Research (CSIR) – Central Leather Research Institute (CLRI), Chennai 600 020, India
[b] Department of Biological Chemistry, Indian Association for the Cultivation of Science, Kolkata 700 032, India
[c] Polymer Science Unit, Indian Association for the Cultivation of Science, Kolkata 700 032, India

HIGHLIGHTS

- Green silver nanoparticles (AgNPs) have been synthesized on the surface of *Rhizopus oryzae*.
- The obtained AgNPs are highly monodisperse and spherical having ~15 nm size.
- The synthesized silver nano-biohybride have been employed for purification of water containing pesticides and microorganisms.
- AgNPs on silver nano-biohybride strongly adsorb organophosphorous pesticides due to soft–soft interaction.
- Rupture of bacterial cell wall occurred after interaction with silver nano-biohybride material.

GRAPHICAL ABSTRACT

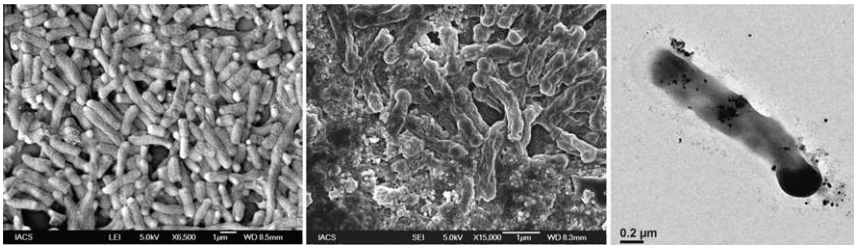

ARTICLE INFO

Article history:
Received 20 June 2012
Received in revised form 16 August 2012
Accepted 19 August 2012
Available online 31 August 2012

Keywords:
Silver nanoparticles
Rhizopus oryzae
Pesticide adsorption
Antibacterial activity

ABSTRACT

A green chemical synthesis of silver nanoparticles (AgNPs) through *in situ* reduction of silver nitrate ($AgNO_3$) by a fungal strain of *Rhizopus oryzae* is described along with the promising eco-friendly role of the synthesized nano-silver bioconjugate (NSBC) material in water purification process. The NSBC has been characterized using UV–vis spectroscopy, high resolution transmission electron (HRTEM) microscopy, and Fourier transform infrared (FTIR) spectroscopy. The NSBC exhibits strong antibacterial activity against *Escherichia coli* and *Bacillus subtilis* and high adsorption capacity towards different organophosphorous pesticides. Fluorescence and electron microscopic images reveal NSBC binds on the bacterial cell wall, which cause irreversible membrane damage eventually leading to cell death. Proteomic analysis further demonstrates down regulation of protein expression, inhibition of cytosolic and membrane proteins and leakage of cellular content following binding of NSBC with bacterial cell wall. NSBC has been exploited to obtain potable water free from pathogens and pesticides in one step process.

1. Introduction

Pesticide contamination in ground water due to indiscriminate use in agricultural practices, poses a serious threat to human health (Zolgharnein et al., 2011). Further the presence of pathogenic bacteria in potable water aggravates the problem (Hillie and Hlophe, 2007). Thus it is an essential prerequisite to reduce the concentration of pesticides to permissible limit and pathogens from potable water but difficult to achieve using conventional treatment technology. Recent advances in nanoscience focus on development of nanotechnology based water treatment methodology (Pradeep and Anshup, 2009). The nanoscale silver materials usually in the range of 1–100 nm in at least one dimension is of

* Corresponding author. Tel.: +91 4424437132; fax: +91 4424911589.
E-mail addresses: sujoy@clri.res.in, sujoydasiacs@gmail.com (S.K. Das).

0960-8524/$ - see front matter © 2012 Elsevier Ltd. All rights reserved.
http://dx.doi.org/10.1016/j.biortech.2012.08.071

great importance and are being increasingly applied to tackle many technological challenges (Perez, 2010; Vaidyanathan et al., 2009). The synthetic protocols for the production of silver nanomaterials (AgNPs) are of paramount importance. Various physical and chemical methodologies that are being followed for the synthesis of AgNPs often raise environmental questions and consequently there is increasing demands for green chemical approach (Dahl et al., 2007; Virkutyte and Varma, 2011). Microorganisms have recently been utilized as living nano factories in order to develop clean, non-toxic and environmentally benign route for metal nanoparticle (MNP) production. Diverse types of microorganism such as bacteria, fungi, algae, and viruses, have been used for the synthesis of MNPs (Das and Marsili, 2010; Das et al., 2012; Mishra et al., 2011; Musarrat et al., 2010; Vaidyanathan et al., 2009). However, filamentous fungus is considered as potential nanofactories because of easy handling procedure, production of large quantity of viable mycelia, high tolerance to metal ions, and well dispersed formation of nanoparticles (Das et al., 2012). The recent research focus is concentrated to find out suitable fungal organism for nanomaterial synthesis with emphasis on improving the rate of production, stability, monodispersity of the products and minimizing the production cost. Very recently, well dispersed and stable shape controlled synthesis of gold nanoparticles have been reported by fungi *Rhizopus oryzae* (Das et al., 2012).

This manuscript describes the green synthesis of AgNPs on the surface of fungal mycelia of *R. oryzae* and application of the obtained silver nano-bioconjugate (NSBC) in the removal of pathogenic bacteria and some model pesticides from water.

2. Experimental

2.1. Materials

The pesticides (purity 98%) were purchased from AccuStandard, INC, USA. Microbiological media and ingredients were procured from HiMedia, India. All the other chemicals and biochemicals were purchased from Merck, Germany.

2.2. Microorganisms

R. oryzae (MTCC 262), *Escherichia coli* (MTCC 062), and *Bacillus subtilis* (MTCC 441) were obtained from the Institute of Microbial Technology, Chandigarh, India. The fungal and bacterial strains were maintained on potato dextrose and nutrient agar slants, respectively.

2.3. Methods

2.3.1. Synthesis of silver nanoparticles on fungal mycelia

Mycelia of *R. oryzae* were obtained by growing the organism in potato dextrose broth (2% potato extract and 2% dextrose) for 3 days at 30 °C under static condition. Following growth, mycelia were harvested and washed with 50 mM phosphate buffer (pH 6.0). Synthesis of AgNPs on the surface of mycelia were carried out by adding blotted dried *R. oryzae* mycelia (0.2 g) to 25 mL aqueous solution (pH 6.0) of $AgNO_3$ containing 100–1000 mg/L silver, and then incubated with shaking (120 rpm) at 30 °C for 72 h. The reduction of Ag^+ was monitored visually and UV–vis spectrophotometrically (Varian CARY 50 Bio). The experiment was repeated by varying pH from 2.0 to 8.0. Control experiments contained no *R. oryzae* mycelia.

2.3.2. Characterization of silver nanoparticles

The formation as well as shape, morphology, and crystal structure of the synthesized AgNPs were characterized using UV–vis spectroscopy, Fourier transform infrared (Shimadzu FTIR spectrometer) spectroscopy, and high resolution transmission electron microscopy (HRTEM, JEOL JEM 2010) equipped with an energy-dispersive X-ray spectroscopic analysis (EDXA).

2.3.3. Antimicrobial activity of NSBC

The antibacterial activity of the dispersed solution (see Supporting information) of NSBC was determined against *E. coli* and *B. subtilis* by cup-plate method as well as by LIVE/DEAD viability assay. The organisms were inoculated in nutrient broth (0.3% beef extract and 0.5% peptone) and incubated at 37 °C for 20 h. The culture cells were harvested by centrifugation; washed with 0.9% saline solution (NaCl) and finally suspended in the saline solution to obtain cell density 10^4 colony forming units (CFU) per mL (see Supporting information). The organisms were individually spread over the surface of the nutrient agar plates and two wells were cut into each plate with a sterile cork borer (0.5 cm diameter). NSBC solution (100 μL) was poured into one well while the other well contained 100 μL of dispersed solution of pristine mycelia as a control. The plates were then kept in a refrigerator for 2 h for diffusion of the test materials and finally incubated at 37 °C for 24 h. The zone of inhibition of bacterial growth was measured. The microbicidal activities of NSBC were determined by staining the cells with LIVE/DEAD viability kit (Invitrogen, CA), containing two DNA-binding stains SYTO 9 and propidium iodide, after incubation with NSBC for 30 min. The excitation/emission maxima for these dyes are approximately 480/500 nm for SYTO 9 stain and 490/635 nm for propidium iodide. The samples were prepared following the manufacturer's instructions and micrographs were recorded on a fluorescence microscope (Olympus BX-61) using an excitation filter of BP460–495 nm. Living and dead cells in the same microscopic fields were viewed separately with different fluorescence filter sets and the cell viability was assayed by counting green (live) and red (dead) cells. The alteration of the cellular morphology following treatment with NSBC was observed using field emission scanning electron microscope (FESEM, JEOL JSM 6700F) and TEM (JEOL JEM 2010) images. The samples were prepared as described earlier (Das et al., 2009).

2.3.4. Protein profile analysis

Freshly grown *E. coli* cells were treated with NSBC solution for 10 h. The cells were collected by centrifugation and suspended in 100 mM phosphate buffer solution (pH 7.2) followed by crushing with sea sand in a motor and pestle at 4 °C. The cell free protein extract (intracellular protein) was collected by centrifugation (10,000 rpm, 15 min) and protein profile was then analyzed by standard 12% sodium dodecyl sulfate–polyacrylamide gel electrophoresis (SDS–PAGE) followed by staining with Coomassie Brilliant Blue R-250 solution. The cell free protein extract of untreated cells served as control. In a separate experiment, the cell free protein extract was treated with NSBC for 10 h. The unbound protein(s) was separated by centrifugation and protein profile was analyzed by SDS–PAGE as described above.

2.3.5. Adsorption of pesticides by NSBC material

The lyophilized (25 mg) pristine mycelia and NSBC were added separately in different 100-mL Erlenmeyer flasks containing 25 mL aqueous solution (100 μg/L pesticides) of parathion, chlorpyrifos, and γ-BHC and incubated at 30 °C (ambient temperature) for 24 h with shaking (120 rpm). The pH of the solution was varied from 2.0 to 7.0. At the end of incubation, adsorbents (pristine mycelia or NSBC) were separated by centrifugation at 10,000 rpm for 15 min and pesticide concentration in the supernatants was measured by gas chromatography (GC, Hewlett–Packard 6890 series) with nitrogen–phosphorous detector. Each experiment was conducted at least three times unless stated otherwise.

2.3.6. Adsorption experiments with simulated water

Organophosphorus pesticide (20 μg/L) and viable *E. coli* cells (10^3 CFU/mL) were added to potable water to prepare contaminated samples. At different time intervals, the concentrations of pesticide and bacteria in the simulated water were determined by GC analysis and MacConkey agar plate method, respectively following treatment with NSBC as described above.

All the experimental details are provided in the Supporting information.

3. Results and discussion

3.1. Synthesis of silver nanoparticles by R. oryzae mycelia

In situ synthesis of AgNPs on the surface of *R. oryzae* mycelia was carried out by incubation of the organism with $AgNO_3$ solution. This led to the formation of AgNPs on the mycelial surface with concomitant change of mycelial color from white to pale yellow and finally deep brown within 72 h. The UV–vis spectra of the dispersed solution of brown mycelia unlike pristine mycelia exhibited an absorption band at about 410 nm due to Surface Plasmon Resonance (SPR) of the AgNPs. The control experiments without mycelia remained colorless. This indicated that the synthesis of AgNPs was mediated by mycelial reduction. The surface coverage of mycelia with AgNPs increased with increasing the initial concentration of silver ions up to 1000 mg/L. The kinetic results (Supporting Fig. S1A) further demonstrated the completion of the reaction within 72 h as the absorption band intensity at 410 nm increased with time and attained saturation value. TEM micrographs (Supporting Fig. S1B) confirmed the synthesis of AgNPs on the mycelial surface. High resolution image (Supporting Fig. S1C) showed the formation well dispersed spherical AgNPs with average diameter of 15 nm. Histogram of the particle size distribution (PSD) measured from 250 nanoparticles in multiple TEM micrographs depicted that average particle size is 15.6 ± 2.5 nm (Supporting Fig. S1D). Most importantly, the as synthesized particles remained stable even after 3 months since the absorption band did not change during this period, indicating that strong interactions between AgNPs and *R. oryzae* prevent aggregation of the synthesized AgNPs. The mycelium decorated with AgNPs was referred to as nano-silver-bioconjugate (NSBC). EDXA spectrum of the NSBC showed a characteristic peak of silver at ~3.0 keV (Supporting Fig. S1E) with additional peaks of carbon, nitrogen and oxygen, which originated from the biomolecules of the mycelia. The selected area electron diffraction (SAED) pattern showed the Scherrer ring patterns (Supporting Fig. S1E, inset) with [111], [200], [222], and [311] atomic planes characteristic of the face centered cubic (fcc) lattice (Das et al., 2012) of nanocrystalline AgNPs. The FTIR spectrum of the pristine mycelia (Supporting Fig. S1F) exhibited strong bands at 3420, 2924, 2852, 1709, 1657, 1533, 1460 and 1412 cm^{-1}, characteristics of amino, carboxyl, hydroxyl, phosphate, and sulfonate groups of proteins, respectively (Das et al., 2009; Wei et al., 2012). The shifting as well as appearance of a new band was observed in the FTIR spectrum of NSBC (Supporting Fig. S1G). The amide I and II bands appeared at 1641 and 1549 cm^{-1}, respectively, in the NSBC. Further, the absorption band at 1641 cm^{-1} was broadened. The shifting of the absorption peak at 1055 to 1078 cm^{-1} and appearance of a new peak at 1063 cm^{-1} confirming phosphate group of lipoprotein was responsible for ecofriendly synthesis of stable AgNPs. The results, therefore, suggested that the mycelial surface acted both as reducing agent as well as template in the *in situ* synthesis of AgNPs. The synthetic process was further repeated at various pH values of the solution between pH 2.0 to 8.0. It was observed that at low pH values (pH < 4.0), the reaction was very slow and took more than 120 h to complete the reaction. On the other hand, at higher pH values (>6.0) the reaction was completed within 60 h. The quantitative elemental analysis of mycelia after 60 h of reaction showed that the yields of synthesized AgNPs were increased at higher pH values compared to that at low pH values. At higher pH values, the mycelia surface carried negative charge (Das et al., 2006) through deprotonation, which facilitated the electrostatic binding of positively charged Ag^+ ions and thereby leading to higher amounts of synthesized AgNPs.

3.2. Antibacterial activity of NSBC

The antimicrobial activity of the dispersed NSBC solution was tested by cup-plate method and LIVE/DEAD viability kit against *E. coli* (gram negative) and *B. subtilis* (gram positive). The dispersed NSBC solution showed strong antimicrobial activity against both the organisms as evident from the clear zone of inhibition around the cup (II) containing this solution (Supporting Fig. S2A–B) whereas no zone of inhibition was observed in the control experiment with dispersed solution of the pristine *R. oryzae* mycelia in the cup (I). The inhibition of bacterial growth by NSBC indicated that the fungal mycelia fabricated with AgNPs become highly antimicrobial. Bacteriocidal activity of NSBC was tested by LIVE/DEAD kit as described in the experimental section. Exposure of *E. coli* to NSBC resulted in significant decrease in cell viability (Supporting Fig. S2D) compared to the cells treated with the dispersed solution *R. oryzae* mycelia (Supporting Fig. S2C). Counting the live (green) and dead (red) bacteria showed significant ($p < 0.1$) reduction (~90%) in the cell viability due to NSBC treatment. This observation established the microbicidal activity of NSBC. SEM micrographs revealed aggregation as well as alteration of cellular morphology on exposure to NSBC. The rod shaped *E. coli* (Supporting Fig. S2E) with relatively smooth cell surface became elongated (Supporting Fig. S2F). The cellular integrity was lost following exposure to NSBC. Moreover, the surfaces of the treated cells were roughened, cracked and ruptured. Accumulation of electron dense AgNPs, throughout the cell wall as confirmed from EDXA spectra was clearly visible in TEM micrographs (Supporting Fig. S2G). In addition, the membranes of the treated cells were damaged severely; many pits and gaps appeared on the cell surface (indicated by arrow in the figure), leading to leakage of cytoplasmic fluids. Similar observation was also noted in *B. subtilis* after exposure to NSBC. The alteration of cellular morphology under stress condition was reported as a defence mechanism (Song et al., 2011). The high redox potential of Ag [$E_H°(Ag^+/Ag^0) = 0.8$ V] caused oxidative decomposition of proteins and lipopolysaccharide molecules following binding of NSBC on bacterial cell wall. This led to increase in membrane permeability, which caused subsequent leakage of the intracellular contents (Li et al., 2010; Song et al., 2011). The protein concentration in the solution following treatment of *E. coli* cells with NSBC increased significantly to 2.1 mg/mL from 0.5 mg/mL for untreated cells. The release of cellular materials due to rupture of cell membrane was observed in *E. coli* following exposure to copper nanoparticle composite material (Mallick et al., 2012). The dimerization of DNA and impairment of electron transport pathway was reported (Feng et al., 2000) on interacting with Ag^+ ions. The effect of NSBC on expression of protein profiles in *E. coli* was further analyzed through SDS–PAGE. Fig. 1 showed considerable change in the intracellular protein profile of NSBC treated cells compared to that of the control *E. coli*. Down-regulation (Lane 3) of proteins was observed in the treated cells. A few bands were missing and band intensities were also lowered in treated samples compared to the control one (Lane 2). The result thus showed that the protein expressions were suppressed due to the toxic effect of AgNPs in NSBC. Leakage of proteins into the solution through cell lysis might also be responsible for lower protein expressions. In a separate

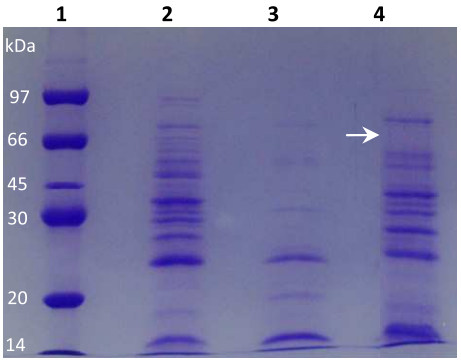

Fig. 1. SDS–PAGE protein profile of control (lane 2) and NSBC treated (lane 3) *E. coli* cell free protein extract. Lane 4 corresponds to unbound proteins following interaction of the protein extract with NSBC. The molecular weight standard is displayed in the far left lane (lane 1).

Table 1
Adsorption of pesticides on the pristine mycelia and NSBC material.

Pesticides	Adsorption (%)	
	Pristine mycelia	NSBC material
Parathion	22.5 ± 2.2	88 ± 4.5
Chlorpyrifos	30.4 ± 3.8	98.4 ± 5.6
γ-BHC	8.2 ± 2.1	15.4 ± 1.8

Data represent an average of five independent experiments.

Table 2
Changes with time in pesticides and *E. coli* concentration in simulated water after NSBC treatment.

Time of incubation (min)	Parathion (μg/mL)	Chlorpyrifos (μg/mL)	*E. coli* (cell/mL)
Control[a]	14.0	6.0	60
5	5.0	2.0	3
10	1.2	N.D[b]	N.D[b]

[a] Control flask received no mycelia.
[b] N.D, not detectable.

experiment the cell free protein extract was incubated with NSBC. The unbound proteins were separated and run into SDS–PAGE. The protein profile of the unbound proteins showed that a few bands were absent (lane 4, indicated by arrow) compared to that of the control protein (lane 2). The strong binding of high affinity proteins (66–45 kDa) to NSBC surface might be led to the disappearance of these protein bands. Previous study (Wigginton et al., 2010, and references therein) also demonstrated that AgNPs strongly bind to different enzymes and non-enzyme proteins including porins, chaperones, or periplasmic peptide-binding proteins thereby inhibiting their activities; probably NSBC was bound to the cellular and membrane proteins following transportation through the compromised cell wall and inhibited their activities ultimately killing the bacteria. These results, therefore, suggested that microbicidal activities of NSBC occurred through multiple steps: (i) toxic of effect of Ag in NSBC down-regulated the protein expressions, (ii) destabilization of the cell membranes through binding of NSBC, which caused pore formation and subsequently induced the leakage of cytoplasmic content and (iii) inhibition of enzyme and protein activities due to binding of NSBC.

3.3. Adsorption of pesticides by NSBC

The adsorptive removal of parathion, chloropyrifos and γ-BHC by NSBC was studied for the development of nanotechnology based water treatment technology. It was interesting to note that the adsorption of organophosphorus (parathion and chloropyrifos) pesticides on NSBC increased significantly to 85–99% compared with the corresponding values of 20–25% for the pristine mycelia (Table 1). However, adsorption of organochlorinated pesticide γ-BHC on NSBC did not change appreciably compared with the pristine one. The adsorption capacities of organophosphorus pesticides increased further with increase in surface coverage of mycelia with AgNPs. The soft–soft interaction (Pearson, 1988) between sulfur atom of pesticides and the silver atoms of NSBC thus favored the binding of organophosphorus pesticides to NSBC but such type of interaction was absent in γ-BHC. No pertinent effect was observed when the experiment was conducted at different pH values clearly demonstrating that covalent binding, instead of electrostatic one was the main driving force in the adsorption of these pesticides on NSBC (Ghosh et al., 2009).

3.4. Treatment of simulated contaminated water with NSBC

The removal of pesticides and bacterial pathogens was carried out from simulated contaminated water relevant to the environmental condition containing *E. coli* and pesticides employing NSBC. The concentrations of the pesticides and *E. coli* density in the treated water decreased significantly within 10 min. *E. coli* could not be detected in the treated water and chloropyrifos level decreased below detectable limit (<1 μg/L), whereas the concentration of parathion (1.2 μg/L) was reduced to the permissible limit (Table 2). The control experiment with the pristine *R. oryzae* mycelia failed to kill *E. coli* and adsorb pesticide appreciably. Time-lapse fluorescence microscopic image of *E. coli* cells during treatment with NSBC revealed that the number of red (dead) cells increase with time and after 10 min of incubation, >90% loss of the cell viability was observed.

4. Conclusions

Silver nanoparticles have been synthesized on the surface of *R. oryzae* by one pot green chemical approach to form NSBC, which exhibits strong antimicrobial activity and adsorption affinity for organophosphorus pesticides. Fluorescence and electron microscopic images demonstrate that the interaction of NSBC with microbial cells causes rupture of the cell membrane resulting in cell death. Proteomic study reveals down-regulation of proteins and leakage of the cytoplasmic contents of *E. coli* on treatment with NSBC through destabilization of the cell wall macromolecules. The proficient antibacterial activity and pesticide adsorption capacity of NSBC suggest that the material may be very useful in water purification technology.

Appendix A. Supplementary data

Supplementary data associated with this article can be found, in the online version, at http://dx.doi.org/10.1016/j.biortech.2012.08.071.

References

Feng, Q.L., Wu, J., Chen, G.Q., Cui, F.Z., Kim, T.N., Kim, J.O., 2000. A mechanistic study of the antibacterial effect of silver ions on *Escherichia coli* and *Staphylococcus aureus*. J. Biomed. Mater. Res. 52, 662–668.
Dahl, J.A., Maddux, B.L.S., Hutchison, J.E., 2007. Toward greener nanosynthesis. Chem. Rev. 107, 2228–2269.
Das, S.K., Das, A.R., Guha, A.K., 2006. Adsorption behavior of rhodamine B on *Rhizopus oryzae* biomass. Langmuir 22, 7265–7272.
Das, S.K., Das, A.R., Guha, A.K., 2009. Adsorption behavior of mercury on functionalized *Aspergillus versicolor* mycelia: atomic force microscopic study. Langmuir 25, 360–366.

Das, S.K., Dickinson, C., Lafir, F., Brougham, D.F., Marsili, E., 2012. Synthesis, characterization and catalytic activity of gold nanoparticles biosynthesized with *Rhizopus oryzae* protein extract. Green Chem. 14, 1322–1334.

Das, S.K., Marsili, E., 2010. A green chemical approach for the synthesis of gold nanoparticles: characterization and mechanistic aspect. Rev. Environ. Sci. Biotechnol. 9, 199–204.

Ghosh, S., Das, S.K., Guha, A.K., Sanyal, A.K., 2009. Adsorption behavior of lindane on *Rhizopus oryzae* biomass: physico-chemical studies. J. Hazard. Mater. 172, 485–490.

Hillie, T., Hlophe, M., 2007. Nanotechnology and the challenge the cleaning of water. Nat. Nanotechnol. 2, 663–664.

Li, W.-R., Xie, X.-B., Shi, Q.-S., Zeng, H.-Y., OU-Yang, Y.-S., Chen, Y.-B., 2010. Antibacterial activity and mechanism of silver nanoparticles on *Escherichia coli*. Appl. Microbiol. Biotechnol. 85, 1115–1122.

Mallick, S., Sharma, S., Banerjee, M., Ghosh, S.S., Chattopadhyay, A., Paul, A., 2012. Iodine-stabilized Cu nanoparticle chitosan composite for antibacterial applications. ACS Appl. Mater. Interfaces 4, 1313–1323.

Mishra, A., Tripathy, S.K., Yun, S.I., 2011. Bio-synthesis of gold and silver nanoparticles from *Candida guilliermondii* and their antimicrobial effect against pathogenic bacteria. J. Nanosci. Nanotechnol. 11, 243–248.

Musarrat, J., Dwivedi, S., Singh, B.R., Al-Khedhairy, A.A., Azam, A., Naqvi, A., 2010. Production of antimicrobial silver nanoparticles in water extracts of the fungus *Amylomyces rouxii* strain KSU-09. Bioresour. Technol. 101, 8772–8776.

Pradeep, T., Anshup, 2009. Noble metal nanoparticles for water purification: a critical review. Thin Solid Films 517, 6441–6478.

Pearson, R.G., 1988. Absolute electronegativity and hardness: application to inorganic chemistry. Inorg. Chem. 27, 734–740.

Perez, D.P., 2010. Silver Nanoparticles. InTech, Croatia.

Song, J., Song, H., Kong, H., Hong, J.-Y., Jang, J., 2011. Fabrication of silica/polyrhodanine core/shell nanoparticles and their antibacterial properties. J. Mater. Chem. 21, 19317–19323.

Vaidyanathan, R., Kalishwaralal, K., Gopalram, S., Gurunathan, S., 2009. Nanosilver – the burgeoning therapeutic molecule and its green synthesis. Biotechnol. Adv. 27, 924–937.

Virkutyte, J., Varma, R.S., 2011. Green synthesis of metal nanoparticles: biodegradable polymers and enzymes in stabilization and surface functionalization. Chem. Sci. 2, 837–846.

Wei, X., Luo, M., Li, W., Yang, L., Liang, X., Xu, L., Kong, P., Liu, H., 2012. Synthesis of silver nanoparticles by solar irradiation of cell-free *Bacillus amyloliquefaciens* extracts and $AgNO_3$. Bioresour. Technol. 103, 273–278.

Wigginton, N.S., Titta, A.D., Piccapietra, F., Dobias, J., Nesatyy, V.J., Suter, M.J.F., Bernier-Latman, R., 2010. Binding of silver nanoparticles to bacterial proteins depends on surface modifications and inhibits enzymatic activity. Environ. Sci. Technol. 44, 2163–2168.

Zolgharnein, J., Shahmoradi, A., Ghasemi, J., 2011. Pesticides removal using conventional and low-cost adsorbents: a review. Clean – Soil, Air, Water 39, 1105–1119.